Ion Mobility and Levitation Effect: Anomalous Diffusion in Nasicon-Type Structure

P. Padma Kumar[†,‡] and S. Yashonath*[,‡,§,#]

Solid State and Structural Chemistry Unit and Supercomputer Education and Research Centre, Indian Institute of Science, Bangalore 560 012, India, and Condensed Matter Theory Unit, Jawaharlal Nehru Centre for Advanced Scientific Research, Bangalore 560 012, India

Received: October 3, 2001; In Final Form: December 21, 2001

A molecular dynamics study of ion mobility as a function of the size of the mobile ion within Nasicon-type structures is reported. The self diffusivity exhibits an anomalous peak suggesting that the levitation effect exists even in ionic systems dominated by Coulomb interaction. This has important consequences in the diffusion of ions in chemical and biological systems. It is seen that high mobility of the ion is associated with the liquidlike radial distribution functions between the ion and the oxygen of the framework. The force on the ion due to the framework within which it is moving is found to be a minimum.

I. Introduction

The subject of diffusion within porous solids has attracted considerable attention from chemists and biologists and, more recently, physicists.[1,2] This subject is of considerable importance because many of the biological, chemical, and physical processes involve diffusion of molecular or ionic species within confined regions or media.[3] There are innumerable materials—some inorganic, others organic—that have interconnected porous space sufficient for small molecules or ions to diffuse.[4] New solids with such pores are often reported.[5,6] Of these, zeolites, which are aluminosilicates, have been studied in some detail, probably because of their importance in catalyzing reactions and separating mixtures of molecules relevant, among others, to the petrochemical industries.[7] Molecules, mainly hydrocarbons, within different zeolites have been investigated by a number of experimental techniques such as IR, uptake, neutron, NMR, etc.[8] More recently, computational methods such as molecular dynamics (MD) and Monte Carlo (MC) have been employed to understand diffusion and other properties within zeolites.[9]

It has been shown through these MD studies that there is a strong dependence of the self diffusivity, D, on the interaction between the diffusing species and the zeolite.[10−12] Such interactions may be characterized by two parameters, σ_{gh} and ϵ_{gh}, when the interactions are assumed to be of (6-12) Lennard-Jones (L-J) form. Under these circumstances, one finds a surprising behavior: the self diffusivity D initially (for small sizes of diffusing species) decreases linearly when plotted against the reciprocal of the square of the size of the diffusing species, $1/\sigma_{gg}^2$, referred to as the linear regime, but at large sizes exhibits a peak often referred to as the anomalous regime (see Figure 1).[12] The effect is referred to as the levitation effect. All studies to date have been carried out on systems in which the predominant interaction between the diffusing species and the porous solid is of Lennard-Jones form. It has been found that a potential with both attractive dispersive and overlap repulsive interactions shows the levitation effect. Simulations with only the repulsive interactions do not exhibit this effect.

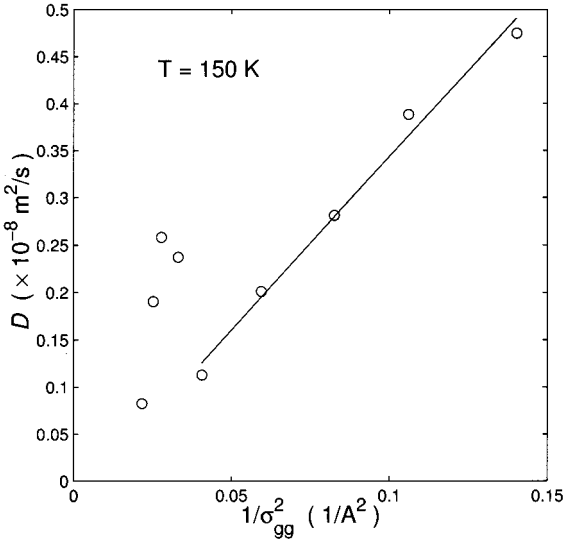

Figure 1. The diffusion coefficient, D (at ∼150 K), as a function of $1/\sigma_{gg}^2$ for zeolite Y, taken from ref 12. A straight line fitted to data points in the linear regime is also shown.

A natural question that would be of interest is whether such behavior would exist in systems dominated by long-range Coulomb interactions. It is not clear whether the anomalous peak would be seen in ionic systems, which are dominated by long-range Coulomb interactions, for the following reasons. One of the conditions for the presence of the anomalous peak in D is that the force on the diffusing species due to the host medium, though significant, sums to zero or nearly zero. This happens because the force on the guest due to the wall on one side is equal but opposite to that due to the wall placed symmetrically opposite. Such a cancellation is possible in systems with short range interactions because locally (in the neighborhood of the guest species) the environment is exactly identical in diagonally opposite directions. It is not at all apparent that such identical environments will exist in opposite directions when the short-range potential is replaced by long-range Coulomb interactions.

* To whom correspondence should be addressed. E-mail: yashonath@sscu.iisc.ernet.in.

† E-mail: padma@sscu.iisc.ernet.in.

‡ Solid State and Structural Chemistry Unit, Indian Institute of Science.

§ Supercomputer Education and Research Centre, Indian Institute of Science.

Jawaharlal Nehru Centre for Advanced Scientific Research.

10.1021/jp013699j CCC: $22.00
Published on Web 03/08/2002

Among the many materials that exhibit ionic conductivity, superionic conductors (SICs) are systems with rather high electrical conductance ($>10^{-3}\ \Omega^{-1}\ cm^{-1}$). These materials find application in solid electrolytes, super capacitors, high-energy-density storage batteries, sensors, etc. A number of factors influence diffusion of ions in solids, and these have been carefully investigated.[13] On the basis of these studies, it has been found that the requirements for a material to be a good SIC are high density of the charge-carrying species, high density of vacant *accessible* sites, and "*smooth*" conducting channels connecting these sites. These factors give rise to a "disordered sublattice" or a "molten sublattice" of the conducting species. In fact, this aspect forms the motivation of the "liquidlike" or "free ion" theories of superionic conductors.[13] There have been several experimental results in the literature that suggest that the size of the ion might affect the ionic mobility: in β-alumina for the conductivity among Li^{+1}, Na^{+1}, Ag^{+1}, K^{+1}, and Rb^{+1} ions, it is seen that the maximum occurs for Na^{+1} ion.[13,14] Later, Wang, Gaffari, and Choi carried out a study of the potential energy surface and related it to conduction mechanism.[15] Their calculation confirmed the existence of a maximum in conductivity for Na^{+1}. Flygare and Huggins[16] also have examined the effect of size of the ion on its activation energy obtained from plots of conductivity against temperature. However, it has not been possible to look at the variation of size of the ion alone in isolation because it is not possible to do this experimentally. Both this and the above-mentioned investigations into the levitation effect call for a detailed study of the effect of ion size on its mobility.

Here, we attempt to answer this by carrying out MD simulations of ions diffusing within Nasicon-type framework structures. We report MD simulations of the variation of self diffusivity, D, and ion mobility of cations diffusing through the voids of a Nasicon-type structure consisting of ZrO_6 octahedra and PO_4 tetrahedra as a function of the size of the cation, σ_M. We have assumed the framework to be rigid. The frequencies associated with the framework motion are generally higher than the those associated with the ion motion. As a result, in all probability, the introduction of framework flexibility will not have any significant influence on the results reported here. Details of the Nasicon structure and interionic potential are presented in the next section.

II. Methods

A. Structure of Nasicon. A brief account on the void (site) structure in Nasicon-type frameworks may be helpful before we discuss the results of the present work. The high-temperature (superionic) phase of Nasicons is rhombohedral and crystallizes in the $R\bar{3}c$ space group.[17−20] The framework consists of corner-shared PO_4 tetrahedra and ZrO_6 octahedra. The structure provides two distinct crystallographic void sites (or simply sites) that could be occupied by the mobile cations of the system. These sites shall be referred to as site 1 (the 6b sites of $R\bar{3}c$) and site 2 (the 18e sites of $R\bar{3}c$).[19−22] Apart from these two, a midcation site, of lower occupancy, has also been observed in some cases.[20,23,24] The distribution of these in a unit cell may be visualized as follows: the six site 1's lie on planes parallel to the *ab* plane (the hexagonal plane) at $c = n/6$, where $n = 1, 2, ..., 6$. The 18 site 2's lie on planes (again, parallel to the hexagonal plane) at $c = n/12$, where $n = 1, 3, ..., 11$ with each plane containing three site 2's arranged at the corners of an equilateral triangle. A site 1 is six-coordinated by the site 2's, and a site 2 is two-coordinated by the site 1's. There are six oxygen atoms around site 1 at a distance of ~2.5 Å. These oxygen atoms form an octahedron ($M(1)O_6$ octahedron). The site 2 is eight-coordinated with oxygen placed in an irregular fashion (four at 2.4 Å, six at 2.65 Å, and eight at 3.05 Å).

TABLE 1: Interaction Potential Parameters between M and Other Atoms of the Framework, Zr, P, and O as Well as M

species (X)	q_X ($\|e\|$)	σ_X (Å)	A_{M-X} (eV)	α_X (Å^3)	n_{M-X}
M	0.5311	0.48−1.13	0.9156	0.0213	11
Zr	0.5496	0.86	0.3963	2.2539	11
P	0.5819	0.31	0.1880	2.1005	11
O	−0.2813	1.21	1.1733	5.2825	9

B. Interionic Potential Function. To carry out molecular dynamics simulations of cation motion within the void made up of ZrO_6 octahedra and PO_4 tetrahedra, a reasonable interionic potential is required. Recently, we have proposed[24] a potential that reasonably reproduces the conductivity of Li^{+1} ions in the SIC phase as well as the normal to SIC transition.

The form of the potential is the same as that originally employed by Rahman et al.[25,26] in their study of AgI and subsequently used in our earlier study[24] of Li^{+1} motion in $LiZr_2(PO_4)_3$. The potential is found to reproduce various aspects of Li^{+1} motion in $LiZr_2(PO_4)_3$, in good agreement with experimental observations. This encourages us to use the same potential for the present study, which involves the effect of the size of the ion on its diffusivity. The potential function is given by

$$U_{M-X}(r) = \frac{q_M q_X}{r} + \frac{A_{M-X}(\sigma_M + \sigma_X)^{n_{M-X}}}{r^{n_{M-X}}} - \frac{\alpha_M q_X^{\,2} + \alpha_X q_M^{\,2}}{2r^4} \quad (1)$$

The parameters in the above potential are charges on various ions (q_X), the strength of the repulsive term (A_{M-X}), the size (ionic radii) of the ions (σ_X), the exponent (n_{M-X}) and finally the polarizabilities (α_X) where X = M, Zr, P, or O. The standard ionic radii of Zr, P, and O are chosen.[27] The radius of the diffusing ions (σ_M) is varied over a range of 0.48−1.13 Å. The structure of the host lattice is chosen[19] to be that of $LiZr_2(PO_4)_3$, with Li^{+1} ions replaced by fictitious cations of varying ionic radii indicated by M. The parameters of the potential are given in Table 1. It will be more realistic to vary the polarizability of the ion in addition to the size. However, a simple calculation of the third term on the right-hand side of eq 1 will show that such a variation leads to only a marginal change in the numerator of this term. Therefore, we have only changed the size of the ion, σ_M.

C. Details of Molecular Dynamics Simulation. Molecular dynamics simulations have been carried out in the micro-canonical ensemble by integrating the equations of motion of M ions, while the other ions (Zr, P, and O) of the host lattice are kept static. The $3 \times 3 \times 1$ or 9 unit cells comprising 972 ions (108 Zr, 162 P, and 648 O ions) in the $R\bar{3}c$ space group with 54 mobile M ions comprise the system on which all simulations have been carried out. Lattice parameters were taken from the X-ray diffraction study:[19] $a = b = 8.847$ Å and $c = 22.24$ Å and $\alpha = \beta = 90°$ and $\gamma = 120°$. Periodic boundary conditions have been employed. Ewald summation technique suitably modified for noncubic simulation cells has been used to compute the Coulomb interactions.[28] The use of the Ewald sum along with a cut-off radius of 11.12 Å leads to an error in the range of 0.07−0.3% in the calculation of interaction energy, and therefore, it is expected that these calculations will be free from finite size effects.

Runs have been carried out for several σ_M values in the range 0.48−1.13 Å with the aspired temperature 850 K. The temper-

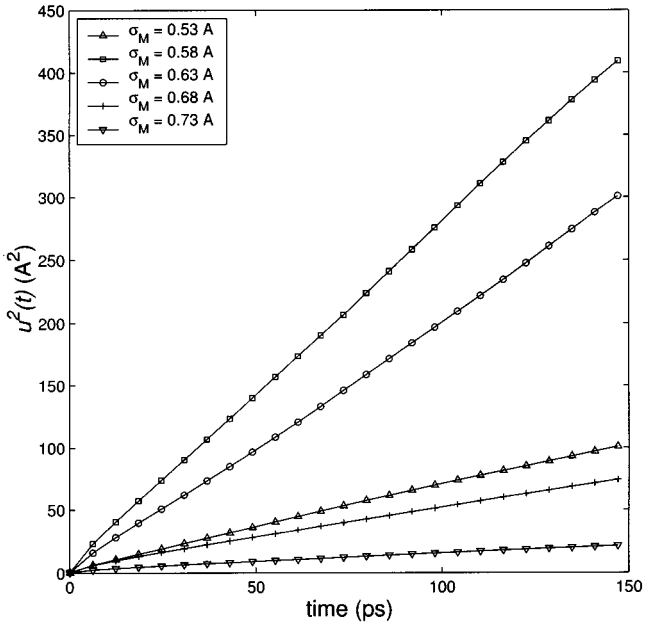

Figure 2. The mean squared displacements, $u^2(t)$, at 850 K as a function of time for various ion sizes in the range 0.53−0.73 Å.

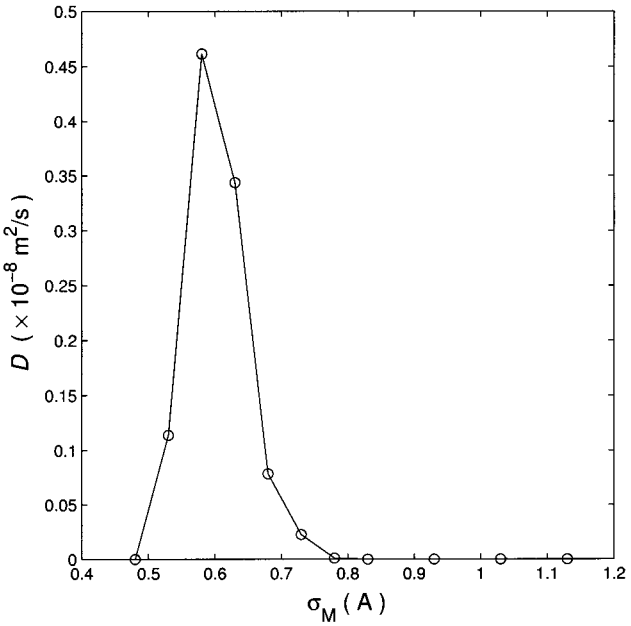

Figure 3. The diffusion coefficient, D, at 850 K plotted against σ_M for $0.48 \leq \sigma_M \leq 1.13$ Å.

ature of the system was adjusted by scaling the velocities.[29] We have ensured that, for all of the runs, the final average temperature of the system is within 4% of the desired value. Velocity Verlet algorithm has been used for integration of MD trajectories.[29] A time step close to 2.5 fs was used to get better control over the temperature. This time step also yielded good conservation in total energy. Equilibration over 300 ps is followed by a run of 600 ps, during which time properties were computed. Positions, velocities, and potential energies of ions were stored every 5 fs for computing properties of interest.

III. Results and Discussion

Figure 2 shows a plot of mean squared displacements, $u^2(t)$, over 300 ps for ions of size 0.53−0.73 Å at a temperature of 850 K. A straight line fitted to $u^2(t)$ between 50 and 100 ps was used to obtain the self diffusivities. A plot of the self diffusivities against σ_M, the size parameter in the intermolecular potential, is shown in Figure 3. It is seen that the self diffusivity is maximum for $\sigma_M = 0.58$ Å. This suggests that an anomalous peak does exist for ion diffusion similar to that reported for atoms diffusing in porous solids such as zeolites. Figure 3 however differs from those found for atom diffusion in porous solids in that there is no regime where $D \propto 1/\sigma_M^2$, in which self diffusivity decreases linearly with increase in σ_M (Figure 1). The reasons for this will be discussed later.

The radial distribution function (rdf), $g(r)$, between the diffusing cations M−M as well as between M−O is shown in Figure 4. First, we note that the M−M $g(r)$ in the case of $\sigma_M = 0.48$ Å exhibits two well-defined peaks located at 6.3 and 9 Å (Figure 4a). With an increase in size to 0.53 Å, it is seen that new peaks appear at lower values of r around 4 and 5.5 Å and also at around 8 Å. For still larger sizes, from 0.58 to 0.68 Å, the $g(r)$ shows only broad peaks suggestive of liquidlike behavior. Similar behavior is seen in the M−O $g(r)$ (Figure 4b). In fact, for $\sigma_M = 0.58$ Å, $g_{M-O}(r)$ shows hardly any peaks beyond 2.5 Å indicative of the liquidlike behavior. These observations suggest that M ions are highly delocalized. This is in agreement with the high self diffusivity (see Figure 3). These findings are in agreement with the free-ion theories, which predict liquidlike behavior of M ions under conditions corresponding to high conductivity.[13]

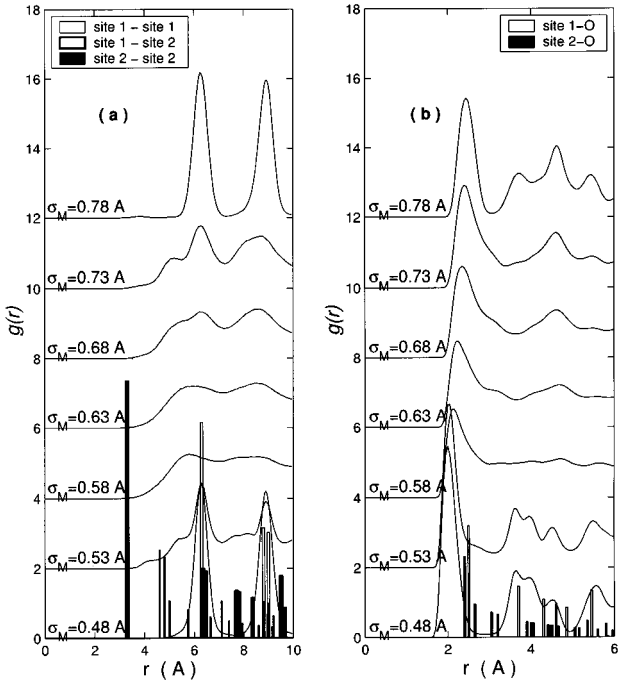

Figure 4. The radial distribution functions, (a) the cation−cation rdf, $g_{M-M}(r)$ and (b) the cation−oxygen rdf, $g_{M-O}(r)$, at 850 K for various ion sizes in the range 0.48−0.78 Å. The vertical lines shown are those corresponding to the X-ray structure without regard to intensity.

Further increase in the size of the ion beyond 0.68 Å leads to a reversal from what is seen so far: the rdf's begin to develop well-defined peaks. For $\sigma_M = 0.78$ Å, two distinct peaks are seen in the M−M $g(r)$ (Figure 4a) at the same positions as those seen for 0.48 Å. The M−O $g(r)$ (Figure 4b) also shows well-defined peaks but is quite different from what was observed for $\sigma_M = 0.48$ Å. The 6.3 as well as 9.0 Å peak in $g_{M-M}(r)$ arises from M ions both located at site 1. This suggests that M ions occupy only site 1 for $\sigma_M = 0.48$ and 0.78 Å at 850 K and contribute negligibly to the self diffusivity. This is in agreement

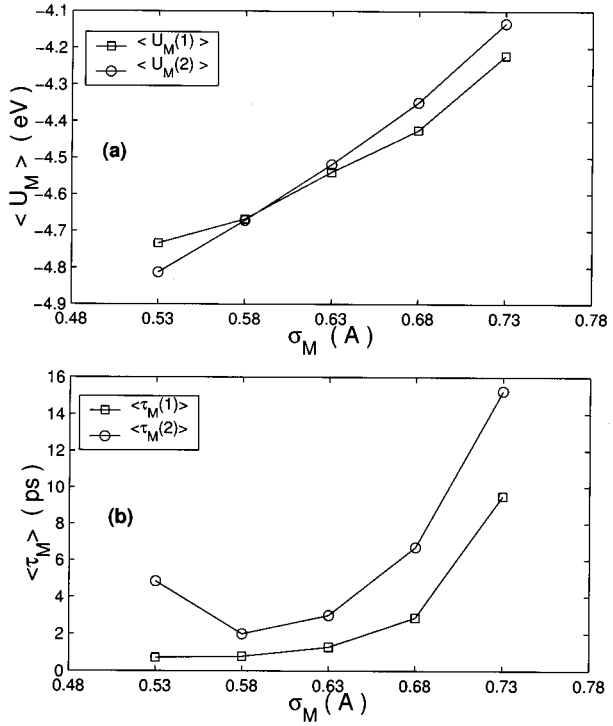

Figure 5. The average (a) potential energies ($\langle U_M \rangle$) and (b) the residence times ($\langle \tau_M \rangle$) of M ions in sites 1 and 2 plotted against σ_M, the ion size.

TABLE 2: The Average Temperatures and Potential Energy of the MD Run for Various Ions and the Total Number of Site−Site Hops Observed in a Run Length of 600 ps

σ_M (Å)	$\langle T \rangle$ (K)	$\langle U_M \rangle$ (eV)	total hops
0.53	855.9	−4.93	3148
0.58	877.0	−4.57	14 630
0.63	860.1	−4.40	12 356
0.68	834.7	−4.25	6316
0.73	866.9	−4.19	2373

with earlier observations on Li^{+1} diffusion for which it was found that, only when Li^{+1} ions occupy site 2, mobility comparable to what is found in SIC phase is obtained.

Table 2 lists the average temperature ($\langle T \rangle$) and the average energy ($\langle U_M \rangle$) of the various M ions from the MD simulation along with the total number of site−site hops observed in a run of length 600 ps. The average energies and residence times of M ions in sites 1 and 2 were obtained by assigning each of the M ions at each of the MD time steps to either site 1 (2, none) if they were within 0.5 Å of site 1 (2, neither). Figure 5a shows a plot of the potential energies of M ions in sites 1 ($\langle U_M(1) \rangle$) and 2 ($\langle U_M(2) \rangle$). A plot of the residence times in sites 1 ($\tau_M(1)$) and 2 ($\tau_M(2)$) is also shown (see Figure 5b). Two interesting points emerge: the self diffusivity is maximum ($\sigma_M = 0.58$ Å) when the difference in the energies between sites 1 and 2 is its least (being nearly zero) and the sum of the residence times in sites 1 and 2 is a minimum.

Figure 6 shows a plot of the energy profile along the path from site 1 to site 2. For all ions except $\sigma_M = 0.58$ Å, the energy profile is rather undulating. The self diffusivity is a maximum for $\sigma_M = 0.58$ Å. This is consistent with Figure 5a in which energies of sites 1 and 2 were found to be comparable. For $\sigma_M \geq 0.63$ Å as also for $\sigma_M \leq 0.53$ Å, undulations increase steadily leading to larger energetic barriers for hops from site 1 to site 2. Because 1−1 and 2−2 hops are only a fraction of 1−2 hops,[21,24,30] the latter are the most important. However, the energy profile along 2−2 hops is also shown (Figure 6b). A

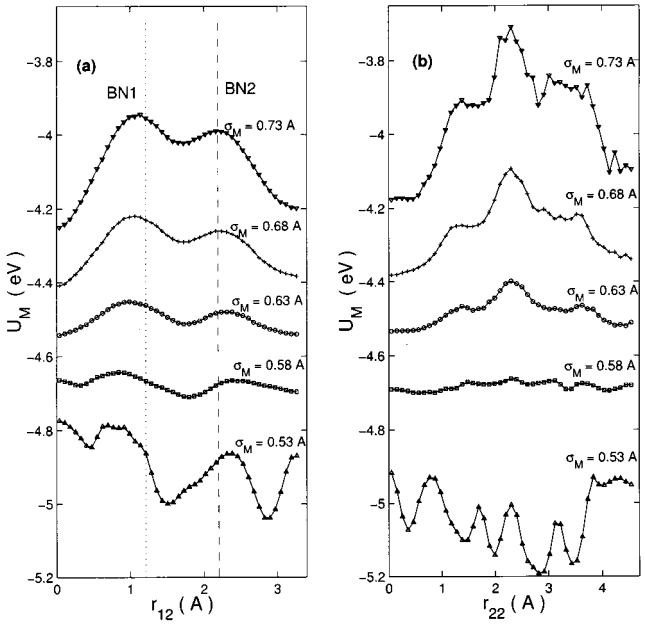

Figure 6. The potential energy profile obtained by averaging over all (a) 1−2 and (b) 2−2 hops of M cations found in the MD simulations at 850 K. The positions of the geometrical bottlenecks for the site 1 to site 2 hop are indicated by a vertical dotted line (for the first bottleneck, BN1) and vertical dashed line (for the second bottleneck, BN2) in panel a.

flat energy landscape appears to be associated with a diffusivity maximum. Similar results[31] were found for different sizes of atoms diffusing in zeolite NaY. Thus, the peak in self diffusivity as a function of the size σ_M is mainly due to the flat potential energy landscape, which leads to lower activation energy. This is one of the characteristics of the levitation effect.[31] Conversely, the peak in the self diffusivity appears to be a consequence of the levitation effect. From Figure 6, it is seen that the potential energy profile for ions of size 0.53 Å during a hop from site 1 to site 2 and from site 2 to site 2 is quite different from those encountered by other ions. This is clear from the rather sharp changes in the energy profile for the 0.53 Å sized ion. This suggests that ions of this size, and also those smaller than this (not shown in Figure 6), are sampling regions of void space that are not sampled by larger ions. This seems to be responsible for the absence of the linear regime that was found in studies of Lennard-Jones atoms within zeolitic voids.[10,11,32] In general, both linear and anomalous regimes are present in systems in which the same void region is sampled by ions or atoms of all sizes.

Yet more evidence that the present maximum in D is in fact a consequence of the levitation effect is a minimum in the net force acting on the sorbate. Figure 7 shows a plot of

$$S = \sum_{l=1}^{L} \sum_{i=1}^{N_M} \bar{F}_i^{l\,2} / (N_M L) \qquad (2)$$

where $\bar{F}_i^l$ is the total force (due to other mobile ions as well as ions constituting the host lattice) on the ith mobile ion at lth MD step. N_M is the number of mobile ions and L is the total number of MD steps. It is seen that for $\sigma_M = 0.58$ and 0.63 Å, the ions with high diffusivity, $S(\sigma_M)$ is small. Earlier, it has been shown that the sum of the force on the guest due to the host will be a minimum for the atom with a maximum in the self diffusivity. In ionic systems, it is difficult to separate the Coulomb contribution due to the guest from those due to the host.

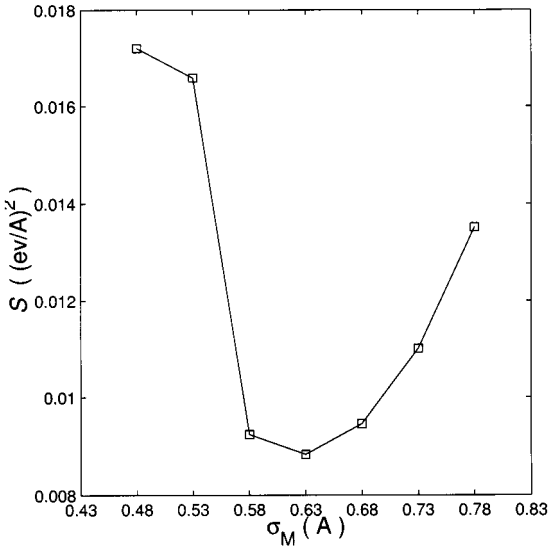

Figure 7. The mean square force, *S*, obtained by averaging over the MD trajectories (see eq 2) for the various sizes (σ_M values) of the diffusing M cations. The dip in *S* around $\sigma_M = 0.58$ and 0.63 Å (the optimal sizes for high diffusion) is indicative of the existence of levitation effect.

Earlier investigations suggest that the peak occurs when the levitation parameter approaches unity.[10] The levitation parameter is defined as

$$\gamma = \frac{2 \times 2^{1/6}\sigma_{gh}}{\sigma_w} \tag{3}$$

where σ_{gh} is the Lennard-Jones interaction parameter between the diffusing species and the atom comprising the host lattice. In the case of zeolites as well as the present case, the latter are the oxygen atoms. Basically, eq 3 is the ratio of the distance at which optimum interaction occurs to that of the size of the window (σ_w, the window diameter). When long-range interactions are present, there is no simple relation between the position at which optimum interactions occur and the pair potential because total interaction is dominated by long-range forces, and therefore, it needs to be modified. The best choice, r_{eq}, is the position of the first peak in M−O $g(r)$. The denominator is the diameter of the bottleneck[21,30,33] defined more precisely as the distance between the centers of the diagonally placed atoms. In the Nasicon structure, there are two bottlenecks for the M ions in their 1−2 hop path (see Figure 8).[21] These bottlenecks are situated at 1.2 and 2.21 Å from site 1. Both of the bottlenecks are formed by triangular arrangement of oxygen atoms in the 1−2 hop path. The first bottleneck, BN1 (the one closer to site 1), is formed by oxygen atoms of the M(1)O_6 octahedra (marked A, B, C in Figure 8). The second bottleneck, BN2 (marked A, B, D in Figure 8), lies closer to site 2 and shares an edge (AB) with the first one. The radius of the bottleneck, σ_w, is defined as the radius of the circle passing through the centers of the three oxygen atoms forming it (the circumradius of the triangle). It is found that, in the present case, both of the bottlenecks have almost the same radius ($\sigma_{w1} = 2.194$ Å and $\sigma_{w2} = 2.199$ Å). It may be seen in Figure 6a that these "geometrical" bottlenecks (their positions are marked by a vertical dotted line for BN1 and a vertical dashed line for BN2) indeed give rise to energetic barriers in the 1−2 hop. The barrier height for BN1 is slightly higher than that for BN2 (Figure 6a). This is probably due to the marginally shorter radius of BN1. The values of r_{eq} and also r_{min}, the position of the minima in the M−O pair potential,

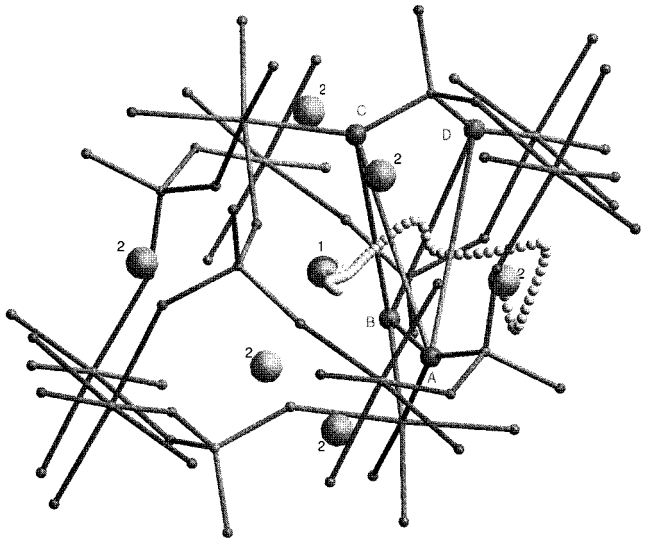

Figure 8. A ball-and-stick view of the $Zr_2P_3O_{12}$ framework as well as the distribution of site 2's (marked 2) within a small sphere around site 1 (marked 1). The oxygen atoms forming the bottlenecks are marked A, B, C, and D and shown slightly larger in size, with triangles A−B−C and A−B−D representing the first and the second bottlenecks, respectively. The radius of the first bottleneck, BN1 ($\sigma_{w1} = 2.194$ Å), is slightly smaller than that of the second bottleneck, BN2 ($\sigma_{w2} = 2.199$ Å). A typical MD trajectory of ions (of size $\sigma_M = 0.63$ Å) from sites 1 and 2 is also shown.

TABLE 3: The Circumradius of the Triangular Bottlenecks (Formed by Oxygen), BN1 and BN2, in the Site 1 to Site 2 Hop Path, $\sigma_{w1} = 2.194$ Å and $\sigma_{w2} = 2.199$ Å, Respectively, and r_{min} and r_{eq}, the positions of the minima of the M−O interaction potential (U_{M-O}) and the first peak positions of the M−O rdf ($g_{M-O}(r)$), respectively

σ_M (Å)	r_{min} (Å)	r_{eq} (Å)	γ (= r_{eq}/σ_{w1})	r_{eq}/σ_{w2}	D ($\times 10^{-8}$ m^2/s)
0.48	1.77	2.00	0.911	0.909	0.0000
0.53	1.85	2.04	0.929	0.927	0.1139
0.58	1.94	2.15	0.979	0.977	0.4615
0.63	2.02	2.27	1.034	1.032	0.3438
0.68	2.11	2.38	1.084	1.082	0.0785
0.73	2.19	2.44	1.112	1.109	0.0227
0.78	2.27	2.47	1.125	1.123	0.0011

along with the self diffusivity, are listed in Table 3. The levitation parameter for ionic systems may be defined as

$$\gamma = \frac{r_{eq}}{\sigma_{w1}} \tag{4}$$

and is also listed. Here, the radius of BN1 is used in defining the levitation parameter, γ, because this is smaller (and corresponds to the highest energy barrier). A plot of *D* against γ is shown in Figure 9. The peak is seen at $\gamma \approx 1$, which suggests that a levitation effect exists.

Figure 10 shows a plot of the power spectra obtained by Fourier transformation of the velocity autocorrelation function, $C(t)$. It is seen that for $\sigma_M = 0.53$ and 0.73 Å as well as 0.68 Å there are rather sharp well-defined peaks. In contrast, sizes of cation that have high self diffusivity are characterized by a broad distribution of frequencies and the absence of any intense peak. Further, the spectrum is relatively flat on the high-frequency side. The presence of a peak toward higher frequency for cation sizes characterized by low diffusivity arises from the vibration of the cation at or near low-energy sites that are usually referred to as adsorption sites (in the present case, sites 1 or 2) or low-energy minima.

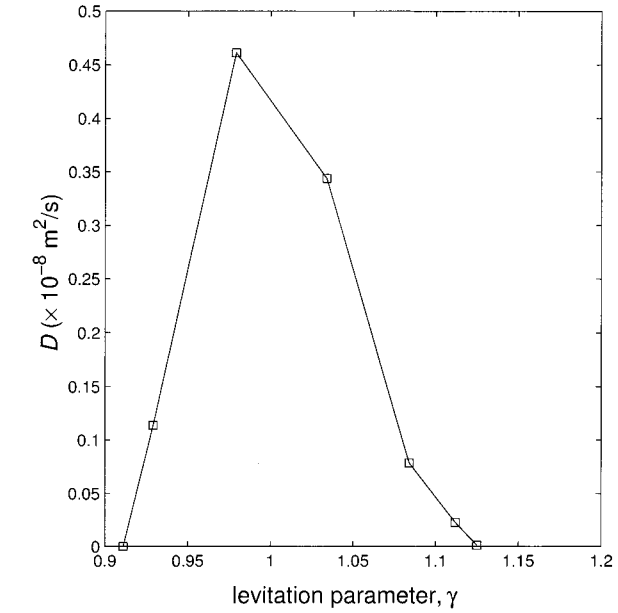

Figure 9. The diffusion coefficient, D, plotted as a function of the levitation parameter ($\gamma = r_{eq}/\sigma_{w1}$). Observe that the peak occurs near $\gamma \approx 1$.

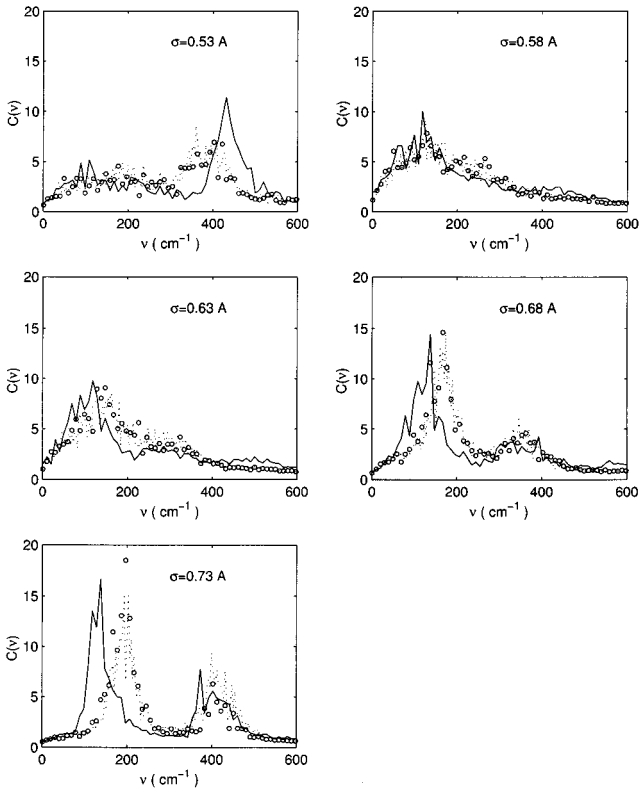

Figure 10. The Fourier transform, $C(\nu)$, of the x- (•••), y- (○), and z- (−) components of the velocity autocorrelation function at 850 K.

IV. Conclusions

A MD study of ion diffusion through the pores of the rigid structure formed by PO_4 tetrahedra and ZrO_6 octahedra suggests that D is a maximum at a particular value of the size of the ion. These results suggest that the levitation effect exists even when the dominant interaction between the ion and the Nasicon framework is long-range. This finding is of considerable importance in many areas: battery materials, ion diffusion across membranes, and sensors among others. The existence of an optimum size for ion diffusion suggests that an ion diffusing through a biomembrane will diffuse faster and with lower activation energy when the size of the channel is optimum. This could provide a way for realizing optimum mobility in complex systems.

Acknowledgment. We are thankful to Professor I. R. McDonald, Trinity College, Cambridge University, for raising the question of existence of levitation effect among ionic solids. We thank the Department of Science and Technology, New Delhi, for financial support through the project "Investigations into Diffusion of Polyatomic Molecules through Porous Media". We wish to acknowledge C.S.I.R., New Delhi, for the award of a fellowship to one of us (P.P.K.). We are thankful to Professor A. M. Umarji for useful discussions regarding Nasicon structure and properties and Professor K. J. Rao for kind encouragement.

References and Notes

(1) *J. Chem. Soc., Faraday Trans. 2* **1991**, *87*, 1947.
(2) Klafter, J.; Drake, J. M. *Molecular Dynamics in restricted geometries*; Wiley: New York, 1989.
(3) Bates, S. P.; vanSanten, R. A. *Adv. Catal.* **1998**, *42*, 1.
(4) Goldberg, I. In *Inclusion Compounds*; Atwood, J. L., Davies, J. E. D., MacNicol, D. D., Eds.; Oxford University Press: New York, 1991; Vol. 4.
(5) Nenoff, T. M.; Chavez, A. J. *Chem. Mater.*, in press.
(6) Gopalakrishnan, J.; Bhuvanesh, N. S. P.; Raju, A. R. *Chem. Mater.* **1994**, *6*, 373.
(7) Barrer, R. M. *Zeolites and Clay Minerals as Sorbants and Molecular Sieves*; Academic Press: London, 1978.
(8) Thomas, J. M. *Philos. Trans. R. Soc. London, Ser. A* **1990**, *333*, 173.
(9) June, R. L.; Bell, A. T.; Theodorou, D. N. *J. Phys. Chem.* **1991**, *95*, 8866.
(10) Yashonath, S.; Santikary, P. *J. Phys. Chem.* **1994**, *98*, 6338.
(11) Yashonath, S.; Santikary, P. *J. Chem. Phys.* **1994**, *100*, 4013.
(12) Sarkar, S.; Anil Kumar, A. V.; Yashonath, S. *J. Chem. Phys.* **2000**, *112*, 965.
(13) Chandra, S. *Superionic Solids*; North-Holland: Amsterdam, 1981.
(14) Kummer, J. T. *Prog. Solid State Chem.* **1972**, *7*, 141.
(15) Wang, J. C.; Gaffari, M.; Sang-il, C. *J. Chem. Phys.* **1975**, *63*, 772.
(16) Flygare, W. H.; Huggins, R. A. *J. Phys. Chem. Solids* **1973**, *34*, 1199.
(17) Hong, H. Y-P. *Mater. Res. Bull.* **1976**, *11*, 173.
(18) Goodenough, J. B.; Hong, H. Y-P.; Kafalas, J. A. *Mater. Res. Bull.* **1976**, *11*, 203.
(19) Petit, D.; Colomban, Ph.; Collin, G.; Boilot, J. P. *Mater. Res. Bull.* **1986**, *21*, 365.
(20) Boilot, J. P.; Collin, G.; Colomban, Ph. *Mater. Res. Bull.* **1988**, *73*, 160.
(21) Kohler, H.; Schulz, H. *Mater. Res. Bull.* **1985**, *20*, 1461.
(22) Kohler, H.; Schulz, H. *Mater. Res. Bull.* **1986**, *21*, 23.
(23) Catti, M.; Stramare, S. *Solid State Ionics* **2000**, *136*−*137*, 489.
(24) Padma Kumar, P.; Yashonath, S. *J. Phys. Chem. B* **2001**, *105*, 6785.
(25) Rahman, A. *J. Chem. Phys.* **1976**, *65*, 4845.
(26) Vashishta, P.; Rahman, A. *Phys. Rev. Lett.* **1978**, *40*, 1337.
(27) Huheey, J. E. *Inorganic Chemistry: Principles of Structure and Reactivity*, 3rd ed.; Harper & Row: Singapore, 1983.
(28) Nosé, S.; Klein, M. L. *Mol. Phys.* **1983**, *50*, 1055.
(29) Allen, M. P.; Tildesley, D. J. *Computer Simulation of Liquids*; Clarendon: Oxford, U.K., 1996.
(30) Kohler, H.; Schulz, H.; Melnikov, O. *Mater. Res. Bull.* **1983**, *18*, 1143.
(31) Chitra, R.; Yashonath, S. *J. Chem. Phys.* **1999**, *110*, 1.
(32) Bandyopadhyay, S.; Yashonath, S. *J. Phys. Chem.* **1995**, *99*, 4286.
(33) Tran Qui, D.; Capponi, J. J.; Joubert, J. C.; Shannon, R. D. *J. Solid State Chem.* **1981**, *39*, 219.